ISSN 2349-7815

International Journal of Recent Research in Electrical and Electronics Engineering (IJRREEE)
Vol. 10, Issue 2, pp: (1-17), Month: April - June 2023, Available at: www.paperpublications.org

A Novel Passive Islanding Detection Method for a Microgrid Using Instantaneous Energy

M.Elshahat Masoud[1], S.Hasan[1], Sherif.S.Saleh[1]*

[1]Electrical Power and Machines Engineering, Helwan University, Helwan, Cairo, Egypt

DOI: https://doi.org/10.5281/zenodo.7810450

Published Date: 08-April-2023

Abstract: **In this paper, a new passive method is proposed to detect islanding of distributed generation using the instantaneous energy that is calculated at the target distributed generation DG or PCC. The instantaneous energy feature can be used to detect islanding status. Instantaneous active energy during Event (IAEDE) and instantaneous reactive energy during event (IREDE) computed from the integration of the Instantaneous active power during the event (IAPDE) and the integration of the instantaneous reactive power during the event (IRPDE). The rate of change of angle (ψ) between them calculated for islanding detection (ROCOψ). The proposed technique has detected the islanding in a rather short time after islanding occurrence. The simulation results showed that the proposed technique could distinguish islanding from other similar events such as load switching at PCC and fault at PCC. This technique can detect islanding efficiently even with zero power mismatches between loads and DGs and hence, reduces the non-detection zone and does not mal operate during similar events. It is more reliable and dependable and the detection time is less than 0.5 sec.**

Keywords: **Distributed generation, Passive islanding detection, Non-Detection Zone, Instantaneous Energy.**

I. INTRODUCTION

The Due to the fast development of the grid, the needs to integrate large-scale renewable energies are immediate priorities and fast emerging issues. The utilization of distributed generations (DGs) will be increased, such as wind energy, solar energy, and fuel cell. The connection of DGs to a power system will raise many challenges, especially protection challenges [1]-[5]. The protection of the microgrid can classify into two types:

A. Traditional protection schemes

It represents schemes used for protection in power systems, for instance, over current protection, earth fault protection, differential protection, over-voltage protection, etc

B. Anti-islanding protection scheme

One of the most important challenges widely discussed over the years is the islanding phenomenon. According to IEEE Std 1547 [6], islanding is defined as a condition in which a part of a power system becomes isolated from the rest of the network and the DG continues to energize part or the entire load.

Islanding affects the safety of the operational staff, who may not realize that a circuit is still powered [7]. It may prevent the automatic re-connection of devices due to an effect on the synchronization of DGs. It effects on the power quality where the grid cannot control the voltage applied to the loads due to the absence of stringent frequency control, leading to abnormal frequencies and voltages. Therefore, the DG should detect islanding quickly and stop energize the area within 2 seconds, according to IEEE Std.1547; this referred to as anti-islanding.

Many types of research have studied islanding detection, which can categorize into three main groups:

1. Local Technique

One This technique is a local algorithm for islanding detection. It can classify into three types:

1.1. Passive Technique

This technique attempts to detect disturbances that occur in the system parameters like voltage, current, frequency, etc. at the DGs site or point of common coupling (PCC) and compare it with reference value [2]-[10]. For instance, under/over voltage protection (UVP/OVP), under/over frequency protection (UFP/OFP), voltage Phase Jump detection (PJD), detection of voltage and current harmonics (THDv), vector surge relays (VSR) and rate of change of frequency (ROCOF). It fast, simple, economical, and do not affect the power quality. It has some drawbacks like having a non-detection zone (NDZ) near-zero power mismatches between DGs and loads

1.2. Active Technique

This technique intentionally introduces disturbances to the system and then monitors the response of the system. If the effect of these small disturbances is significant, it means that the DG islanded, whereas the effect will be negligible when the DG connected to the grid [11]-[19], for instance sliding mode frequency shift (SMS), active frequency drift (AFD), Sandia Frequency shift (SFS), Sandia voltage shift (SVS) and impedance measurement. It reduces the NDZ, but its effects on the power quality and may cause instability. It also has low performance in the existence of multiple DGs.

1.3. Hybrid Technique

This technique is based on the combination of passive and active techniques to take advantage of the passive and active techniques and to eliminate their shortcomings. The active technique performed when islanding is suspected by the passive technique [20]-[28], For instance the slip mode frequency shift (SMS) and ROCOF, Sandia frequency shift (SFS) and ROCOF and voltage unbalance (VU) and high frequency (HF) impedance. It has a small NDZ and low effect on power quality, but its response time is longer than the active technique.

2. Remote Technique

This method is based on communication between utilities and DGs, the basic idea of this scheme is to monitor the state of the DGs, it identifies the areas that are islanded and sends the appropriate signal to the DGs, either to stay in operation or to shutdown [29]-[36], For instance the power line signalling scheme and transfer trip scheme. It is more reliable than local methods, but the cost of equipment and reconfiguration of settings when adding a new component or taking it from the network are the main drawbacks of these methods. In addition, signal distortion can lead to misoperation.

The previous researches found most of the algorithms which were used in the islanding detection still suffer from some problems. So, a new algorithm is proposed to overcome past issues.

This paper proposes a new islanding detection technique based on the instantaneous energy that calculated at targeted distributed generation (DG). The feature of this energy can be used to detect islanding. One of the goals of this paper is to reduce NDZ as much as possible. This paper is organized to cover the proposed scheme and achieve design objectives as follows: Section 2 presents the proposed method for islanding detection. Section 3 provides validation of the performance and feasibility of the proposed anti-island protection scheme. Section No.4 presents comparison between the proposed technique and other old technique. Finally, conclusions stated in section No.5.

II. PROPOSED METHODOLOGY

A. Modelling of Test System

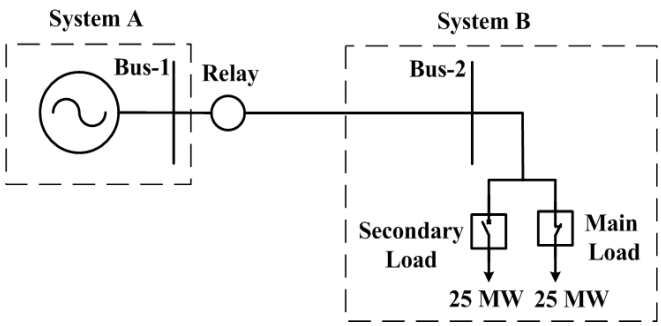

Fig. 1: Test Circuit for MATLAB Simulation.

ISSN 2349-7815

International Journal of Recent Research in Electrical and Electronics Engineering (IJRREEE)
Vol. 10, Issue 2, pp: (1-17), Month: April - June 2023, Available at: www.paperpublications.org

A model of a small electrical network was made using Matlab software as shown in Fig.1. This model consists of the main network (the grid) and two loads, one of them is the primary load and the other is the secondary load, which is switching on at 0.1 sec to clarify the idea which the proposed technique was based on.

B. Proposed technique concept

The proposed technique is based on the use of the instantaneous power generated at the moment of islanding, which has characteristics different from that generated in other normal conditions. To calculate the instantaneous power generated during the event, the incremental quantities will be used as a current signal and voltage signal [37]-[41].

Thus, the instantaneous active power during event IAPDE(t) equation can be written as:

$$IAPDE(t)=\Delta i(t)\ \Delta v(t) \quad (1)$$

The instantaneous reactive power during event IRPDE(t) equation can be written as:

$$IRPDE(t)=\Delta i(t)\ \Delta v(t)\backslash \quad (2)$$

Where:

$$\Delta x(t)=x(t)-x(t-T)\ ,\ x=i, v\ ,\ T=\frac{1}{f} \quad (3)$$

$$\Delta x(t)\backslash=\Delta x\left(t-\frac{\pi}{2}\right)\ ,\ x=v \quad (4)$$

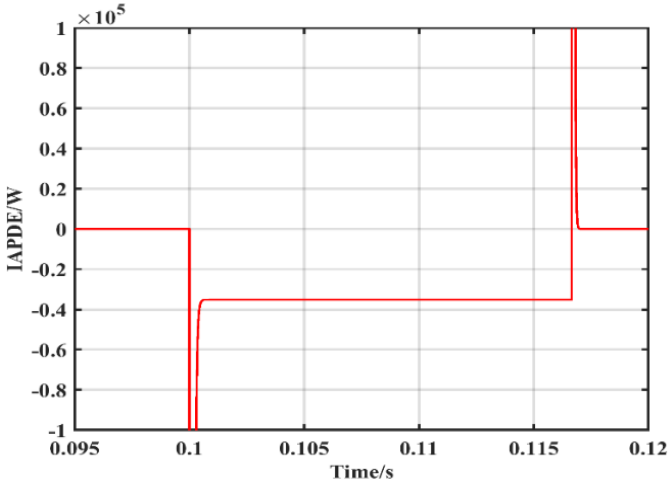

Fig. 2: Instantaneous active power during event.

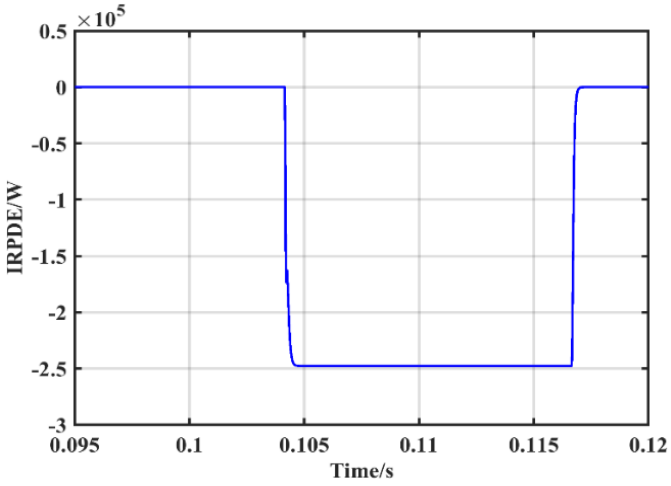

Fig. 3: Instantaneous reactive power during event.

ISSN 2349-7815

International Journal of Recent Research in Electrical and Electronics Engineering (IJRREEE)
Vol. 10, Issue 2, pp: (1-17), Month: April - June 2023, Available at: www.paperpublications.org

The instantaneous active energy during event IAEDE(t) and the instantaneous reactive energy during event IREDE(t) are calculated by the integration of the instantaneous active power during event IAPDE(t) and the instantaneous reactive power during event IRPDE(t), respectively. IAEDE(t) and IREDE(t) can be written as:

$$IAEDE(t)=\int_0^t IAPDE(t)\,dt \qquad (5)$$

$$IREDE(t)=\int_0^t IRPDE(t)\,dt \qquad (6)$$

It will be clear that the values of the steady-state instantaneous power and the instantaneous energy are close to zero as shown in Fig.2, Fig.3, Fig.4 and Fig.5. However, when event happened, the instantaneous power has a value, and instantaneous energy appears.

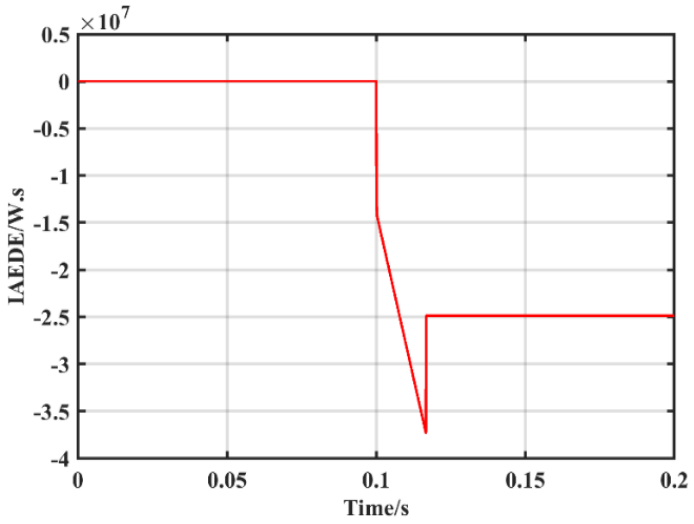

Fig. 4: Instantaneous active energy during event.

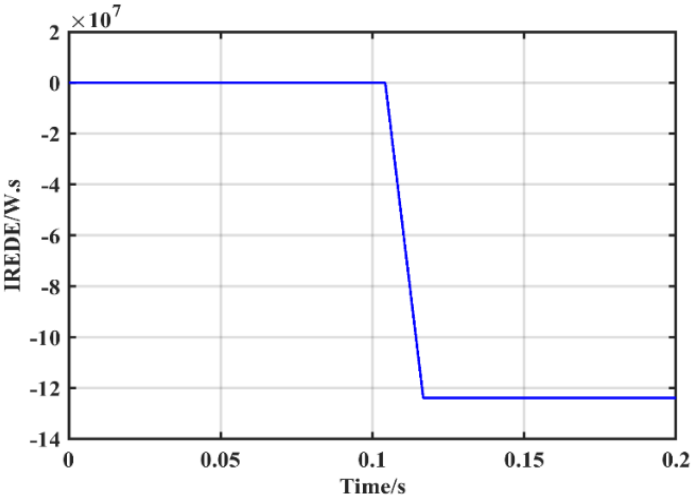

Fig. 5: Instantaneous reactive energy during event.

Although the existing load is a resistive load, instantaneous reactive power appeared because it relies on the incremental quantities without regard to the nature of the load.

The angle (ψ) between the instantaneous active energy and the instantaneous reactive energy during event is shown in Fig.6. It is noted that the angle had changed when the event occurred.

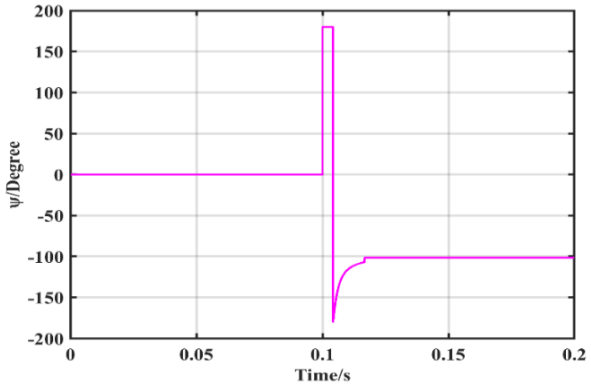

Fig. 6: Angle between IAEDE and IREDE.

The rate of change of angle (ROCOψ) between IAEDE and IREDE is shown in Fig.7, it will be seen that the ROCOψ is affected by the event occurrence in the power system network.

It will become clear later in the third part that the rate of change of angle (ROCOψ) between IAEDE and IREDE is affected by the type of event.

This method does not imply dependence on the angle of the power factor because this angle based on the ratio of the real power absorbed by the load to the apparent power flowing in the circuit, but this method depends on the instantaneous energy during event which not affected by nature of the load Therefore, this explains why the ψ is almost zero in the normal case, and changes as a result of change of power system parameter.

Fig.8 shows the power factor angle. It is noted that the angle not changed when the event occurred.

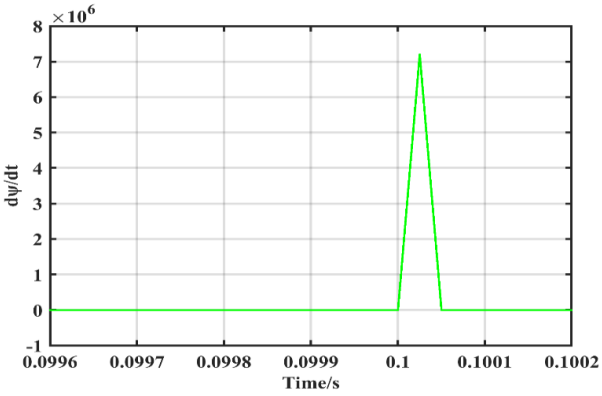

Fig. 7: Rate of change of ψ.

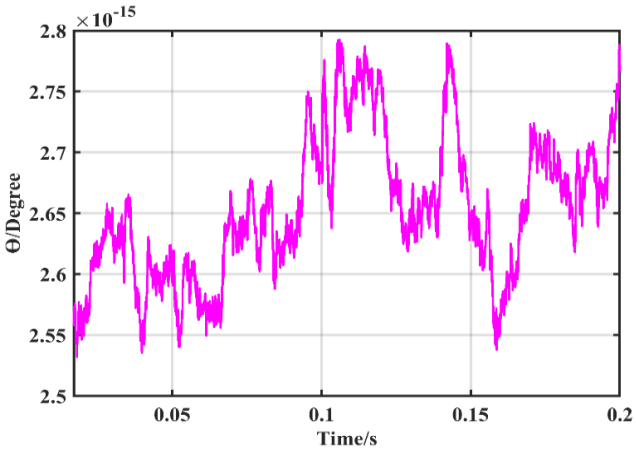

Fig. 8: Angle between voltage and current Θ.

C. Proposed Technique Algorithm

This algorithm relies on the magnitude and the duration of the rate of change of the angle between the instantaneous active energy during event (IAEDE) and the instantaneous reactive energy during event (IREDE). when islanding happened, instantaneous active power appears, and instantaneous reactive power appears also. The magnitude and the duration of them are considerable and long. For normal operation such as load injecting and fault, the instantaneous energy is also appeared. However, the magnitude and the duration of them are inconsiderable and short. The magnitude and the duration of the rate of change of angle (ROCOψ) between the instantaneous active energy during event (IAEDE) and the instantaneous reactive energy during event (IREDE) is the variable that represents the change in both. By the appropriate setting for magnitude and duration of ROCOψ, the islanding can be detected.

By using digital filter (Chebyshev) to remove high frequencies components that make the relay takes a wrong decision [42]-[46].

The poles of the filter can be obtained from this equation:

$$\mathrm{Spx} = -\sinh(\mathrm{A})\sin(\mathrm{B}) + \mathrm{j}\cos(\mathrm{A})\cos(\mathrm{B}) \quad (7)$$

Where:

$$\mathrm{A} = \frac{1}{\mathrm{r}}\sinh^{-1}\left(\frac{1}{\mathrm{c}}\right) \quad (8)$$

$$\mathrm{c} = \sqrt{10^{\frac{\mathrm{ripple}}{10}} - 1} \quad (9)$$

$$\mathrm{B} = \frac{\pi}{2}\frac{2x-1}{\mathrm{r}} \quad (10)$$

x is the pole number, ripple=0.001 and filter order(r)=3.

The transfer function of the filter can be written as:

$$\mathrm{H(s)} = \frac{a_1 s^3 + a_2 s^2 + a_3 s + a_4}{b_1 s^3 + b_2 s^2 + b_3 s + b_4} \quad (11)$$

Where:

$a_1 = a_2 = a_3 = 0, a_4 = 16.4743$

$b_1 = 1, b_2 = 4.8926, b_3 = 12.7188, b_4 = 16.4743$

The all of input signals can be written as:

$$\mathrm{v}(\mathrm{t_y}) = \mathrm{h(t)} * \mathrm{v(t)} \quad (12)$$

$$\mathrm{i}(\mathrm{t_y}) = \mathrm{h(t)} * \mathrm{i(t)} \quad (13)$$

Where:

h(t) represent the impulse response of the filter.

$\mathrm{t_y}$ represent the filter time delay.

IAEDE(t) and IREDE(t) can be rewritten as:

$$\mathrm{IAPDE}(\mathrm{t_y}) = \Delta \mathrm{v_a}(\mathrm{t_y})\,\Delta \mathrm{i_a}(\mathrm{t_y}) + \Delta \mathrm{v_b}(\mathrm{t_y})\,\Delta \mathrm{i_b}(\mathrm{t_y}) + \Delta \mathrm{v_c}(\mathrm{t_y})\,\Delta \mathrm{i_c}(\mathrm{t_y}) \quad (14)$$

$$\mathrm{IRPDE}(\mathrm{t_y}) = \Delta \mathrm{v_a}\backslash(\mathrm{t_y})\,\Delta \mathrm{i_a}(\mathrm{t_y}) + \Delta \mathrm{v_b}\backslash(\mathrm{t_y})\,\Delta \mathrm{i_b}(\mathrm{t_y}) + \Delta \mathrm{v_c}\backslash(\mathrm{t_y})\,\Delta \mathrm{i_c}(\mathrm{t_y}) \quad (15)$$

IAEDE and IREDE can be rewritten as follows:

$$\mathrm{IAEDE}(\mathrm{t_y}) = \int_0^{\mathrm{t}} \mathrm{IAPDE}(\mathrm{t_y})\,\mathrm{dt} \quad (16)$$

$$IREDE(t_y)=\int_0^t IRPDE(t_y)\,dt \qquad (17)$$

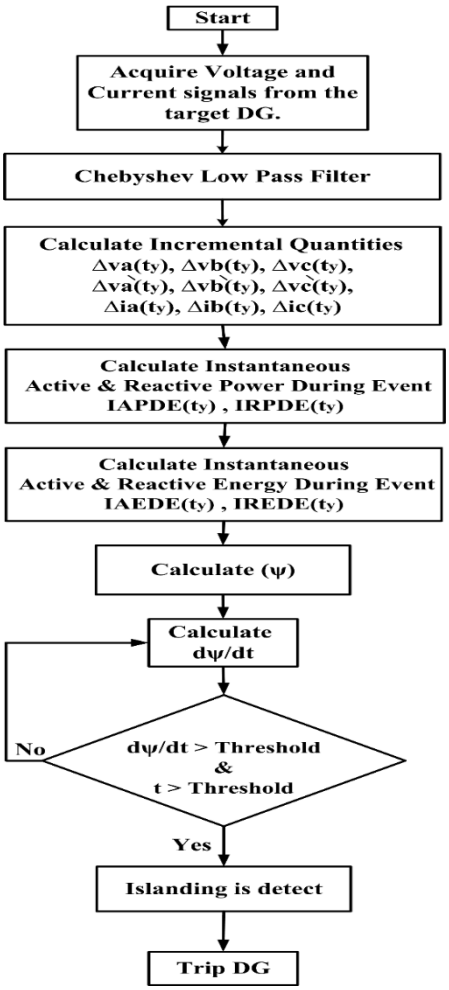

Fig. 9: The flowchart of the proposed strategy for islanding detection.

The angle between the instantaneous active energy during event (IAEDE) and the instantaneous reactive energy during event (IREDE) can be deduced as follows:

$$\psi=\tan^{-1}\left(\frac{IREDE(t_y)}{IAEDE(t_y)}\right) \qquad (18)$$

The ROCOψ are calculated as follows:

$$ROCO\psi=\frac{d\psi}{dt} \qquad (19)$$

ROCOψ is a parameter which is used to detect islanding situation. The flowchart of the proposed technique is shown in Fig.9.

III. PERFORMANCE OF THE PROPOSED TECHNIQUE

In order to verify the efficiency of the proposed technique, three simulation scenarios are designed:

Scenario 1: Islanding with different loads

This Scenario consists of six cases:

Case 1 (power mismatch=25%): PL%=125, QL%=0

Case 2 (power mismatch=0%): PL %=100, QL %=0

Case 3 (power mismatch=0.12%): PL %=100, QL %=5

Case 4 (power mismatch=-50%): PL %=50, QL %=0

Case 5 (power mismatch=-49.75%): PL %=50, QL %=5

Case 6 (power mismatch=-75%): PL %=25, QL %=0

Where:

P% is the active load power percentage from the generated power (15 MVA).

Q% is the reactive load power percentage from the generated power (15 MVA).

Positive power mismatch means that Pload >PDG, negative power mismatch means that Pload <PDG and zero power mismatch means that Pload =PDG

Scenario 2: Load Switching

This Scenario consists of three cases:

Case 1: inject additional load, it is 100% of generated power (15 MVA).

Case 2: reject additional load, it is 100% of generated power (15 MVA).

Case 3: switching of capacitor (1 MVAR).

Scenario 3: Grid Fault

This Scenario consists of four cases:

Case 1: solid single line to ground fault at PCC.

Case 2: high resistance single line to ground fault at PCC.

Case 3: line to line fault at PCC

Case 4: three phase to ground fault at PCC

A. Threshold selection

Table I: Maximum value of ROCOψ which lasts for 30 ms.

		ROCOψ	
		Single Distributed Generator	Multiple Distributed Generators
Non-islanding events	A-G fault	0.00	0.01
	A-G fault & Rf=200 Ω	0.00	0.00
	B-C fault	-0.02	-0.01
	ABC-G fault	0.88	0.88
	Load Inject	2.40	14.81
	Load Reject	0.00	0.00
	Switching of capacitor	0.00	0.00
Islanding events	Positive Power Mismatch (Case 1)	348.96	344.17
	Zero Power Mismatch (Case 2)	258.07	277.71
	Positive Power Mismatch (Case 3)	335.25	275.64
	Negative Power Mismatch (Case 4)	184.10	176.94
	Negative Power Mismatch (Case 5)	168.03	179.08
	Negative Power Mismatch (Case 6)	50.08	20.06

To perform appropriate discrimination between non-islanding cases and islanding situation, selection of the setting is important. Therefore, large numbers of islanding and non-islanding cases, have been simulated in Matlab Simulink as shown in Table I.

The choice of setting depends on two parameters, the value of ROCOψ threshold and the time that signal keep value over than this threshold to bypass the short transient time.

It will be seen from Table 1 that the maximum value of ROCOψ for single distributed generator network during all non-islanding cases remain well below 2.4 and lasts for 30 ms.

It will be seen also from Table 1 that the maximum value of ROCOψ for multiple distributed generator network during all non-islanding events remain well below 14.81 and lasts for 30 ms.

It can be noted from Table 1 that the minimum and maximum value of ROCOψ change between -0.01 to 14.81. Hence, considering safety margin, the threshold (ROCOψ) value of 15 is selected and the time value for keep this signal over than this threshold is 30 ms for correct discrimination between islanding situation and non-islanding conditions.

As can be observed, there are a big difference between the values of the ROCOψ in cases of islanding and in cases of non-islanding, regardless of the type of network. But a study of the ROCOψ has been done to find out the maximum value that the ROCOψ reaches in the cases of islanding events, which is much lower in the normal conditions.

B. Performance with Single DG

To test the performance of the proposed technique, a simulation was carried out using Matlab software on the circuit shown in Fig.10 this circuit consists of a diesel generator connected to the grid through a transformer and circuit breaker No.1. Circuit breaker No.3 is used for islanding condition and circuit breaker No.2 is used for load switching. all scenarios happened at 4 sec and the system frequency is 60 HZ. to identify the islanding, the detection signal must keep value over than (15) for at least (30) ms to trigger signal to circuit breaker No.1.

Islanding is made by disconnecting the circuit breaker No.3.

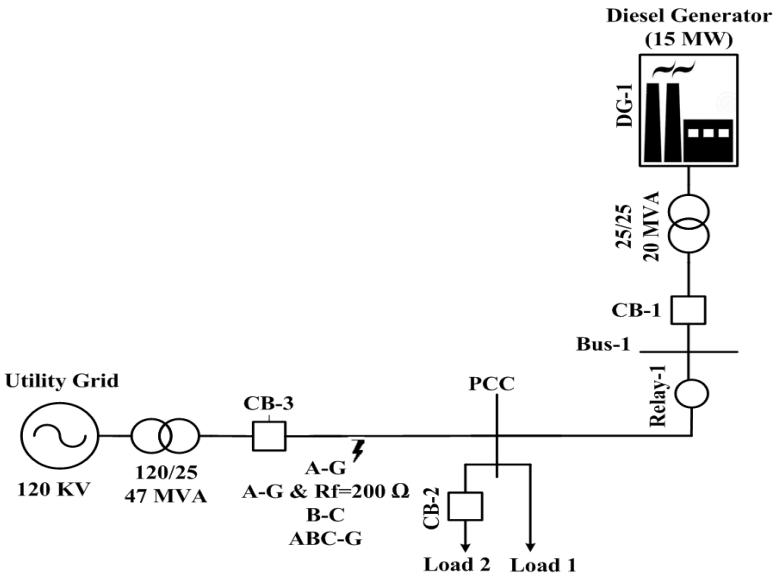

Fig. 10: Single line diagram of the test circuit.

1. Scenario 1 (Load Variation Test)

Fig.11 shows the magnitude of ROCOψ for the six cases that mentioned before. It will be clear that the detection signal equal to zero before the event occurs but it has a significant value after islanding happened. This value increases by increasing power mismatch where the magnitude of ROCOψ for positive power mismatch is greater than the magnitude of ROCOψ for zero power mismatch and the magnitude of ROCOψ for zero power mismatch is greater than the magnitude of ROCOψ for negative power mismatch.

Fig.12 shows close up view of ROCOψ for load variation test to show the trip points.

Table II shows the trip instant time, detection time and ROCOψ. The relay can detect all islanding events in a short time, about less than 100 ms. but in the last case, where the power mismatch is large, the relay takes longer time, where it reached 235 ms.

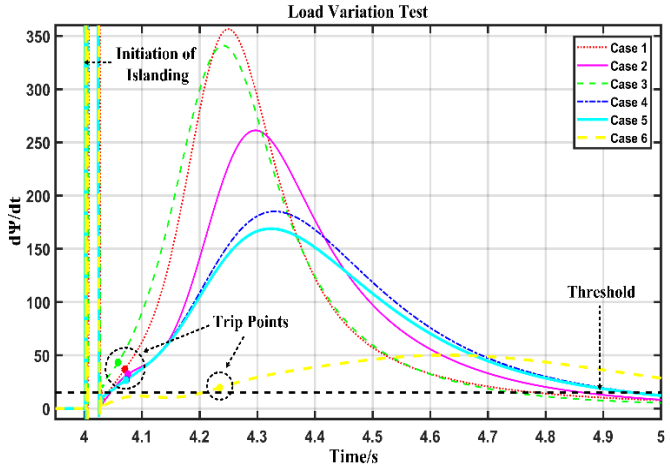

Fig. 11: ROCOψ for load variation test.

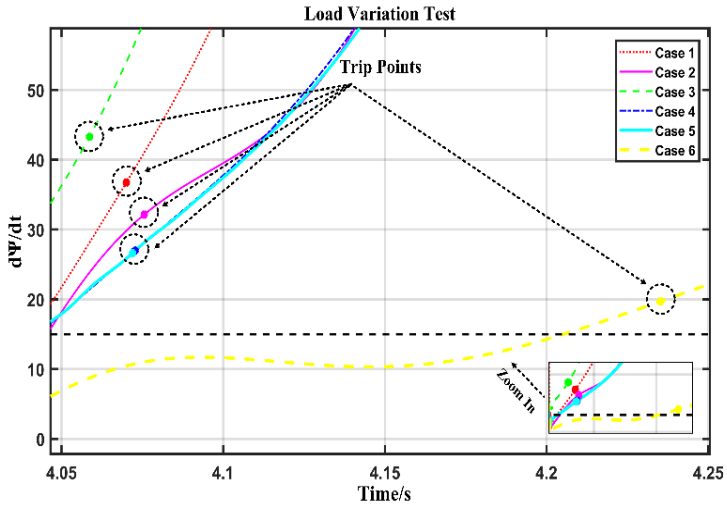

Fig. 12: Closely view of ROCOψ for load variation test.

Table II: Simulation results of the proposed technique.

Case	Trip Instant Time	Detection Time	ROCOψ
1	4.070	70.050	36.736
2	4.076	75.575	32.142
3	4.059	58.625	43.281
4	4.073	72.775	26.983
5	4.072	71.950	26.623
6	4.235	235.225	19.712

2. Scenario 2 (Load Switching Test)

Fig.13 shows the magnitude of ROCOψ for the three cases that mentioned before. It is noted that the magnitude of ROCOψ has a small value in the inject load case, the reject load case and the switching of capacitor case as compared to islanding scenarios, and this value not reach to the threshold value. The detection signal (ROCOψ) at event instant moves over than the detection value but does not keep enough time for trip signal.

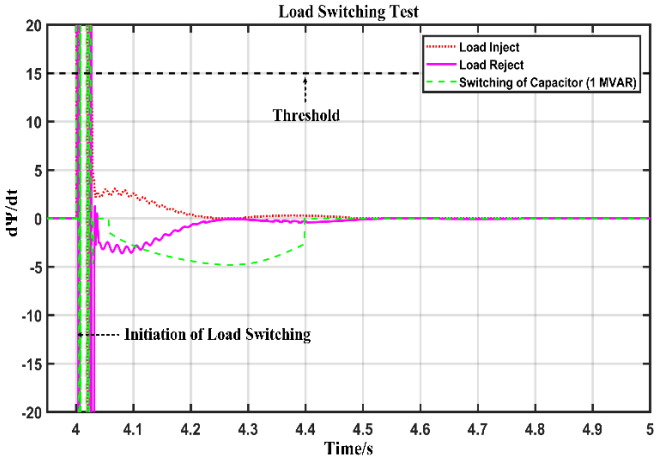

Fig. 13: ROCOψ for load switching test.

3. Scenario 3 (Grid Fault Test)

Fig.14 shows the magnitude of ROCOψ for four cases that mentioned before. It will be seen that the magnitude of the detection signal has a small value in the all fault types as compared to islanding scenarios and this value not reach to the threshold value. The detection signal (ROCOψ) at event instant moves over than the detection value but does not keep enough time for trip signal.

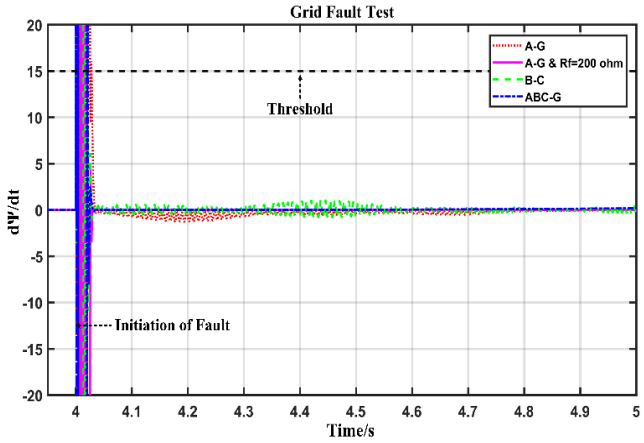

Fig. 14: ROCOψ for grid fault test.

C. Performance with Multiple DGs

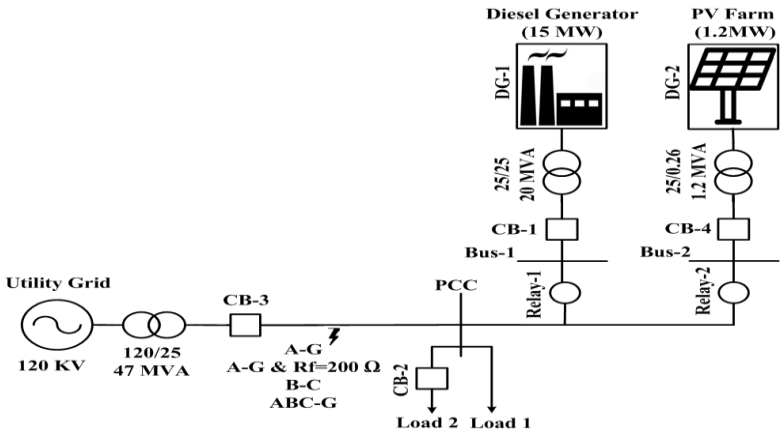

Fig. 15: Single line diagram of the test circuit.

In this section, the performance of the proposed technique will be tested on a network containing two distributed generators as shown in Fig.15. Referring to Fig.10, another DG (PV Farm) will be added to the system in order to work in parallel with the first DG (Diesel generator). PV farm consists of twelve PV arrays delivering 1.2 MW at 1000 W/m2 sun irradiance.

The three scenarios that mentioned before will be applied on the new system to test the relay performance.

1. Scenario 1 (Load Variation Test)

Fig.16 shows the magnitude of ROCOψ for six cases that mentioned before. It will be seen that the detection signal equal to zero before the event occurs but it has a considerable value after islanding happened. This value increases by increasing power mismatch where the magnitude of ROCOψ for positive power mismatch is greater than the magnitude of ROCOψ for zero power mismatch and the magnitude of ROCOψ for zero power mismatch is greater than the magnitude of ROCOψ for negative power mismatch.

Fig.17 shows close up view of ROCOψ for load variation test to show the trip points.

Table III shows the trip instant time, detection time and ROCOψ. The relay can detect all islanding events in a short time, about less than 100 ms. but in the last case, where the power mismatch is large, the relay takes longer time, where it reached 500 ms

Table III: Simulation results of the proposed technique.

Case	Trip Instant Time	Detection Time	ROCOψ
1	4.091	90.750	43.550
2	4.070	70.050	44.262
3	4.071	71.375	48.063
4	4.064	64.375	36.438
5	4.063	63.325	35.870
6	4.441	440.875	15.642

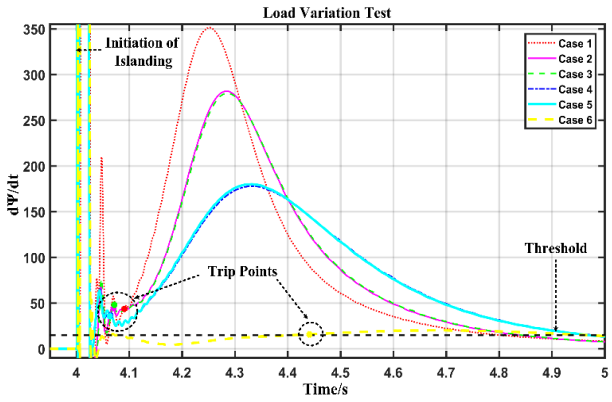

Fig. 16: ROCOψ for load variation test.

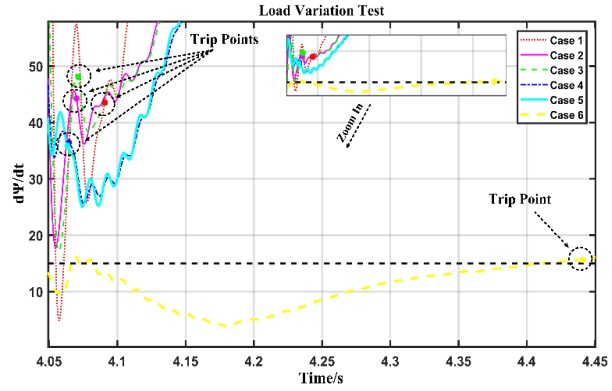

Fig. 17: Closely view of ROCOψ for load variation test.

ISSN 2349-7815

International Journal of Recent Research in Electrical and Electronics Engineering (IJRREEE)
Vol. 10, Issue 2, pp: (1-17), Month: April - June 2023, Available at: www.paperpublications.org

2. Scenario 2 (Load Switching Test)

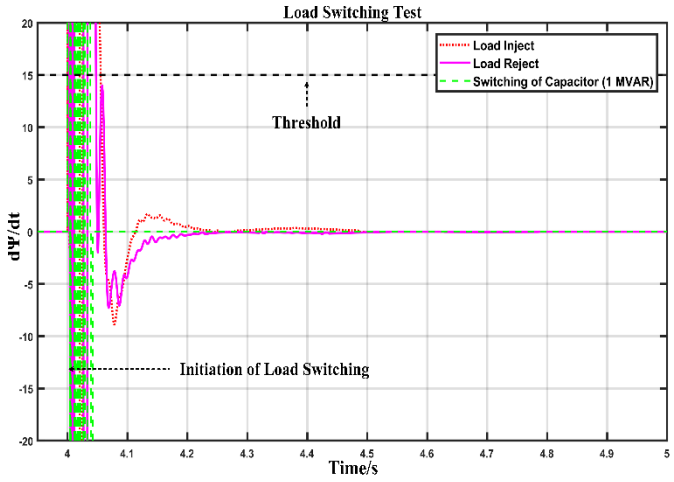

Fig. 18: ROCOψ for load switching test.

Fig.18 shows the magnitude of ROCOψ for the three cases that mentioned before. It will be clear that the magnitude of ROCOψ has a small value also in the inject load case, the reject load case and the switching of capacitor as compared to islanding scenario, and this value not reach also to the threshold value. The detection signal (ROCOψ) at event instant moves over than the detection value but does not keep enough time for trip signal.

3. Scenario 3 (Grid Fault Test)

It is noted that the magnitude of the detection signal has a small value also in the all fault types as compared to islanding scenario, and this value not reach also to the threshold value as shown in Fig.19. The detection signal at event instant moves over than the detection value but does not keep enough time for trip signal.

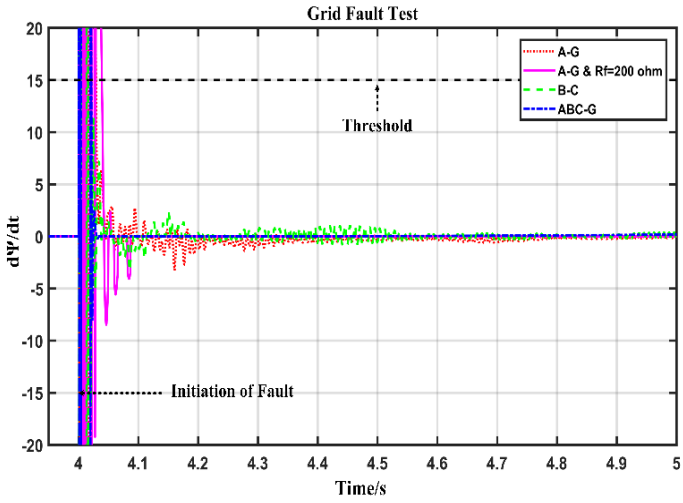

Fig. 19: ROCOψ for grid fault test.

IV. COMPARING THE PROPOSED TECHNIQUE WITH OTHER USED

In the last section, the proposed technique will be compared with another used technique to show its performance [3]. The ROCOF relay measures the generator voltage and estimates Δf/Δt and then computes the average value for every 4 consecutive cycles (Average ROCOF) and checks whether it is lower than the pre-set value and, if so, the output signal will be sent and the circuit breaker will trip to stop islanding. The pickup value is set to -2 Hz/s with the operating time 0.1 s. If the relay became more sensitive by adjusting its threshold to minimize the NDZ, it will identify some other events as an islanding situation.

The performance of the conventional method is evaluated as shown in Fig. 20 and Tables IV, according to the islanding conditions mentioned in Section No.3. As can be observed, the conventional method does not recognize the case 4, case 5 and case 6 as an islanding situation.

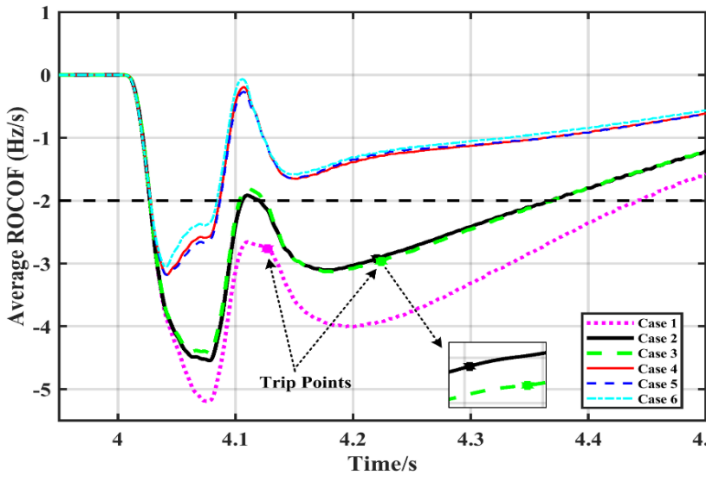

Fig. 20: ROCOF waveforms due to different power mismatches.

Table IV: Simulation results of the ROCOF technique.

Case No.	Power Mismatch %	Trip Instant Time (sec)	Detection Time (ms)	Notes
1	25.00	4.1273	127.3000	
2	0	4.2203	220.3250	
3	0.12	4.2240	224.0250	
4	-50.00			Fail to Operate
5	-49.75			
6	-75.00			

V. DISCUSSION

A detailed study was conducted on this proposed technique to clarify its effectiveness, and this study contains two different models, the first model is a single DG connected to the network and the second model is a multiple DG connected to the network. In the first model simulation was made for two main cases, the first case representing an islanding state and the second case representing normal conditions that occur in the network. As for the first simulation case which is the case of islanding, the study of islanding cases was conducted on a large scale to clarify the effectiveness of the proposed technique in detecting islanding state. The cases of islanding were studied starting from a power mismatch equal to 25 until a power mismatch equal to -75, which is considered one of the worst cases that can occur where the generator capacity is higher than the load power. The proposed technique was able to distinguish all cases within 100 ms. But in the case where the power mismatch is equal to -75, the technique was able to distinguish it despite the difficulty of its occurrence, but in a longer time within 200 ms.

As for the second simulation case, which represents the cases that occur in the network and it is not considered islanding state such as: load switching on, load switching off, capacitor switching on, single line to ground fault, single line to ground fault with high resistance, line to line fault and three phase fault. The proposed technique succeeded in dealing with these cases and did not give any false trip. One of the drawback of this method is the appearance of some instantaneous values of ROCOψ at the beginning of the event and it was overcome by adding value of time setting in order to avoid the occurrence of a false trip.

As for the second model which represents a multiple DG connected to the network, the same previous simulations were applied, and the proposed technique succeeded in detecting all islanding state and not giving any wrong decision in the other cases.

VI. CONCLUSION

In this paper, a new method of islanding detection technique is proposed, to avert the shortage of the islanding techniques, for instance, malfunction, and large NDZ. During islanding, instantaneous energy is created; this energy characteristic can be used to detect an islanding situation. ROCOψ can be used efficiently to distinguish the islanding from other events. The proposed technique has determined the islanding situation in a rather short time after event occurrence, even in 0.07-0.5 sec. It also tested for different cases; the result shows that it can distinguish the islanding in all cases. And also, can detect islanding even 0% power mismatch. It has fast speed operation with reliability and dependability.

REFERENCES

[1] IEEE Std. 1547 (2003). "IEEE Standard for Interconnecting Distributed Resources." Electric Power Systems

[2] Raza S, Mokhlis H, Arof H, Laghari JA, Mohamad H (2016). "A Sensitivity Analysis of Different Power System Parameters on Islanding Detection." IEEE Transactions on Sustainable Energy 7(2):461 – 470.

[3] Chan CY, Lau TK, Ng SK (2015). "An impact study of ROCOF relays for islanding detection." IET 10th International Conference on Advances in Power System Control, pp. 1 - 6.

[4] Ghanem A, Rashed M, Sumner M, Elsayes MA, Mansy II (2017). "Grid impedance estimation for islanding detection and adaptive control of converters." IET Power Electronics 10(11):1279 – 1288.

[5] Singh MS, Jena P, Kumar J, Satsangi S (2016). "Islanding detection using Hilbert Transform in a distributed generation environment." IEEE International Conference on Electrical Power and Energy Systems, pp. 351 – 354.

[6] Liu N, Diduch C, Chang L, Su J (2015). "A Reference Impedance-Based Passive Islanding Detection Method for Inverter-Based Distributed Generation System." IEEE Journal of Emerging and Selected Topics in Power Electronics 3(4):1205 – 1217.

[7] Khamis A, Xu Y, Dong ZY, Zhang R (2018). "Faster Detection of Microgrid Islanding Events Using an Adaptive Ensemble Classifier." IEEE Transactions on Smart Grid 9(3):1889 – 1899.

[8] Abd-Elkader AG, Saleh SM, Eiteba MB (2018). "A passive islanding detection strategy for multi-distributed generations." ELSEVIER on International Journal of Electrical Power & Energy Systems 99, pp. 146 – 155.

[9] Jia K, Bi T, Liu B, Thomas D, Goodman A (2014). "Advanced islanding detection utilized in distribution systems with DFIG." ELSEVIER on International Journal of Electrical Power & Energy Systems 63, pp. 113 – 123

[10] Ghanem A, Rashed M, Sumner M, Elsayes MA,Mansy II (2017). "Grid impedance estimation for islanding detection and adaptive control of converters." IET Power Electronics 10(11):1279 – 1288.

[11] Guo Z (2015). "A harmonic current injection control scheme for active islanding detection of grid-connected inverters." IEEE International Telecommunications Energy Conference.

[12] Hamzeh M, Rashidirad N, Sheshyekani K and Afjei E (2016). "A New Islanding Detection Scheme for Multiple Inverter-Based DG Systems." IEEE Transactions on Energy Conversion 31(3):1002 – 1011.

[13] Cheng Y, Zhao L, Luo Y, Hu C, Rui T, Qi X (2016). "A new method of islanding detection based on voltage positive feedback." IEEE 11th Conference on Industrial Electronics and Applications, pp. 2261–2264.

[14] Gupta P, Bhatia RS and Jain DK (2017). "Active ROCOF Relay for Islanding Detection." IEEE Transactions on Power Delivery 32(1):420 – 429.

[15] Mohammadpour B, Pahlevaninezhad M, Kaviri SM and Jain P (2016). "A New Slip Mode Frequency Shift Islanding Detection Method for single phase grid connected inverters." IEEE 7th International Symposium on Power Electronics for Distributed Generation Systems.

[16] Sun Q, Guerrero JM, Jing T, Vasquez JC, Yang R, (2017). "An Islanding Detection Method by Using Frequency Positive Feedback Based on FLL for Single-Phase Microgrid." IEEE Transactions on Smart Grid 8(4):1821 – 1830.

[17] Jia K, Wei H, Bi T, Thomas DW, Sumner M (2017). "An Islanding Detection Method for Multi-DG Systems Based on High-Frequency Impedance Estimation." IEEE Transactions on Sustainable Energy 8(1), pp. 74 – 83.

[18] Emadi A, Afrakhte H, Sadeh J (2016). "Fast active islanding detection method based on second harmonic drifting for inverter-based distributed generation." IET Generation, Transmission & Distribution 10(14):3470 – 3480.

[19] Wang S, Zhang S, Liu L, Jia Y, Qie C (2016). "An improved active frequency drift anti-islanding detection method." IEEE 11th Conference on Industrial Electronics and Applications, pp. 2170 – 2173.

[20] Akhlaghi S, Sarailoo M, Akhlaghi A Ghadimi AA (2017). "A novel hybrid approach using sms and ROCOF for islanding detection of inverter-based DGs." IEEE Power and Energy Conference at Illinois.

[21] Khodaparastan M, Vahedi H, Khazaeli F, Oraee H (2017). "A Novel Hybrid Islanding Detection Method for Inverter-Based DGs Using SFS and ROCOF." IEEE Transactions on Power Delivery 32(5):2162 - 2170.

[22] Mohanty SR, Kishor N, Ray PK and Catalo JP (2015). "Comparative Study of Advanced Signal Processing Techniques for Islanding Detection in a Hybrid Distributed Generation System." IEEE Transactions on Sustainable Energy 6(1):122 – 131.

[23] Dhar S, Dash PK (2016). "Harmonic Profile Injection-Based Hybrid Active Islanding Detection Technique for PV-VSC-Based Microgrid System." IEEE Transactions on Sustainable Energy 7(4):1473 – 1481.

[24] Murugesan S, Murali V, Daniel SA (2018). "Hybrid Analyzing Technique for Active Islanding Detection Based on d-Axis Current Injection." IEEE Systems Journal 12(4):3608 - 3617.

[25] Ahmadipour M, Hizam H, Othman ML, Radzia MA, Chirehc N (2018). "A novel islanding detection technique using modified Slantlet transform in multi-distributed generation." ELSEVIER on International Journal of Electrical Power & Energy Systems 12(4):3608 – 3617.

[26] Shrivastava S, Jain S, Nema RK, Chaurasia V (2017). "Two level islanding detection method for distributed generators in distribution networks." ELSEVIER on International Journal of Electrical Power & Energy Systems 87, pp. 222 - 231.

[27] Ghzaiel W, Ghorbal MJ, Belkhodja IS, Guerrero JM (2017). "Grid impedance estimation based hybrid islanding detection method for AC microgrids." ELSEVIER on Mathematics and Computers in Simulation 131(4):142 - 156.

[28] Xu YK, He JH, Hu J and Yip HT (2016). "An islanding detection method for inverter-interfaced distributed generation using an adaptive power disturbance approach." IET 13th International Conference on Development in Power System Protection, pp. 1 - 6.

[29] Yang F, Xia N, Han QL (2017). "Event-Based Networked Islanding Detection for Distributed Solar PV Generation Systems." IEEE Transactions on Industrial Informatics 13(1):322 – 329.

[30] Bayrak G and Kabalci E (2016). "Implementation of a new remote islanding detection method for wind–solar hybrid power plants." ELSEVIER on Renewable and Sustainable Energy Reviews 58, pp. 1 - 15.

[31] Bayrak G (2015). "A remote islanding detection and control strategy for photovoltaic-based distributed generation systems." ELSEVIER on Energy Conversion and Management 96, pp. 228-241.

[32] Etxegarai A, Eguía P, Zamora I (2011). "Analysis of Remote Islanding Detection Methods for Distributed Resources." International Conference on Renewable Energies and Power Quality 1(9):1142-1147.

[33] Yin J, Chang L, Diduch C (2004). "Recent Developments in Islanding Detection for Distributed Power Generation." IEEE Large Engineering Systems Conference on Power Engineering, pp. 124-128 .

[34] Dob B and Palmer C (2018). "Communications assisted islanding detection Contrasting direct transfer trip and phase comparison methods." IEEE 71st Annual Conference for Protective Relay Engineers.

[35] Bayrak G and Cebeci M (2014). "A Communication Based Islanding Detection Method for Photovoltaic Distributed Generation Systems." International Journal of Photoenergy 2014(272497):1 – 17.

[36] Cataliotti A, Cosentino V, Nguyen N, Russotto P, Cara DD, Tinè G (2013). "Hybrid passive and communications-based methods for islanding detection in medium and low voltage smart grids." IEEE 4th International Conference on Power Engineering, Energy and Electrical Drives,pp. 1563 - 1567.

[37] Peng FX, Lai JS (1996). "Generalized Instantaneous Reactive Power Theory for Three-Phase Power Systems." IEEE Transactions on Instrumentation and Measurement 45(1):293-297.

[38] Furuhashi T, Okuma S, Uchikawa Y (1990). "A Study on the Theory of Instantaneous Reactive Power." IEEE Transactions on Industrial Electronics 37(1):86-90.

[39] Kong X, Yuan Y, Huang H, Wang Y (2015). "Overview of the instantaneous reactive power theory in three-phase systems." IEEE 5th International Conference on Electric Utility Deregulation and Restructuring and Power Technologies, pp. 2331-2336.

[40] Xianzhong, Liu G, Gretsch R (2004). "Generalized theory of instantaneous reactive quantity for multiphase power system." IEEE Transactions on Power Delivery 19(3):965-972.

[41] Afonso JL, Freitas, Sepulveda MJ, Martins JS (2003). "p-q Theory power components calculations." IEEE International Symposium on Industrial Electronics, pp. 385-390.

[42] Diniz PS, da Silva EA, Netto SL (2010). "Digital Signal Processing: System Analysis and Design." Second Edition, Cambridge University Press,

[43] Chitode JS (2009). "Digital Signal Processing." Third Edition, Technical Publications.

[44] Lathi BP, Green RA (2014). "Essentials of Digital Signal Processing." Cambridge University Press.

[45] Winder S (2002). "Analog and Digital Filter Design Second Edition." Newnes.

[46] Chen WK (2009). "Passive, Active, and Digital Filters." Second Edition, CRC Press.